DOI: 10.1002/asia.201000641

Synthesis and Spectroscopic Properties of Fused-Ring-Expanded Aza-Boradiazaindacenes

Hua Lu,[a, b] Soji Shimizu,[b] John Mack,[b] Zhen Shen,*[a] and Nagao Kobayashi*[b]

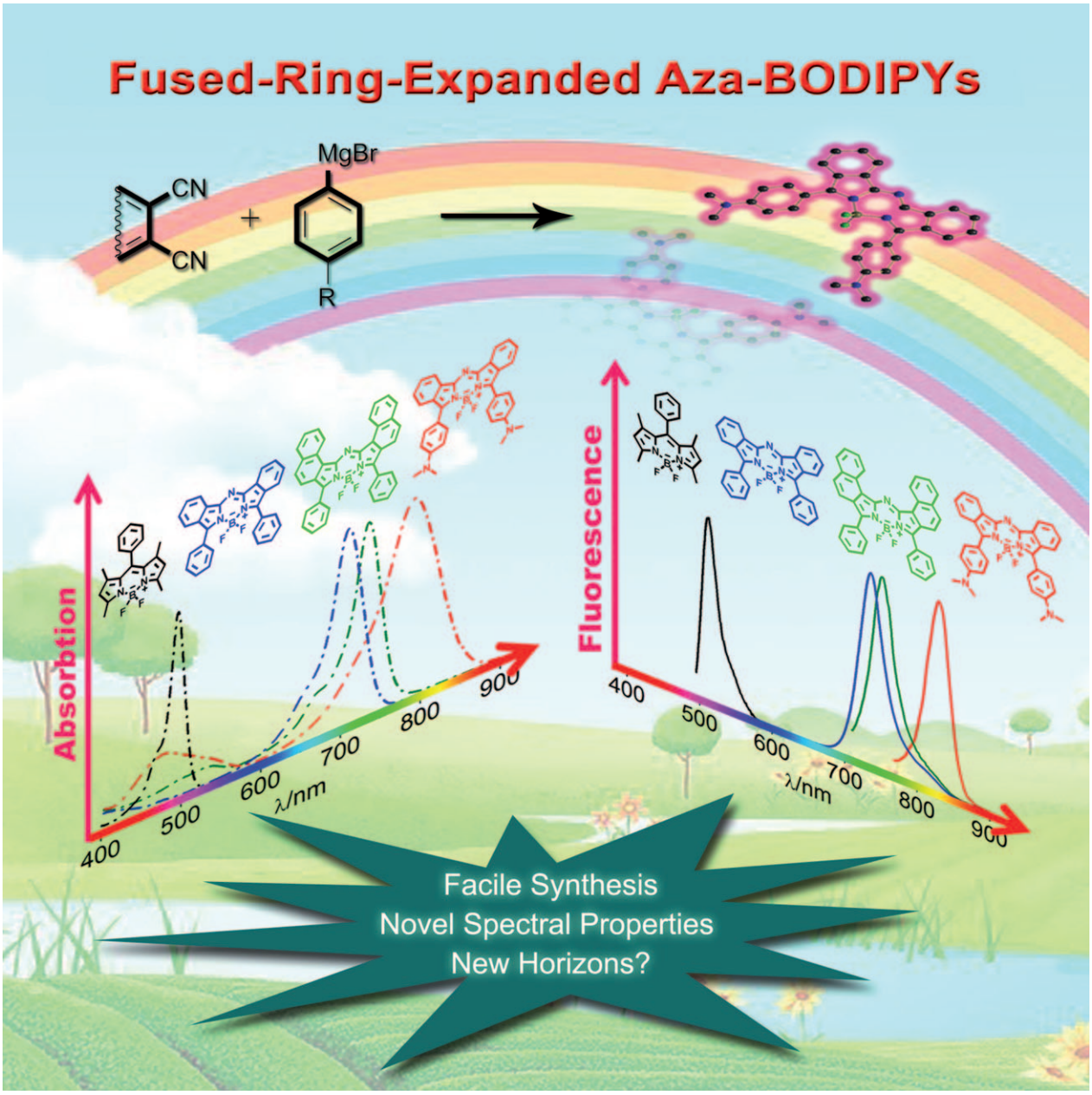

Abstract: A series of fused-ring-expanded aza-boradiazaindacene (aza-BODIPY) dyes have been synthesized by reacting arylmagnesium bromides with phthalonitriles or naphthalenedicarbonitriles. An analysis of the structure–property relationships has been carried out based on X-ray crystallography, optical spectroscopy, and theoretical calculations. Benzo and 1,2-naphtho-fused 3,5-diaryl aza-BODIPY dyes display markedly red shifted absorption and emission bands in the near-IR region (>700 nm) due to changes in the energies of the frontier MOs relative to those of 1,3,5,7-tetraaryl aza-BODIPYs. Only one 1,2-naphtho-fused aza-BODIPY of the three possible isomers is formed due to steric effects, and 2,3-naphtho-fused compounds could not be characterized because the final BF_2 complexes are unstable in solution. The incorporation of a $-N(CH_3)_2$ group at the *para*-positions of a benzo-fused 3,5-diaryl aza-BODIPY quenches the fluorescence in polar solvents and results in a ratiometric pH response, which could be used in future practical applications as an NIR "turn-on" fluorescence sensor.

Keywords: BODIPYs · density functional theory · dyes/pigments · fluorescence · IR spectroscopy

Introduction

Over the past decade there has been considerable interest in the synthesis of organic chromophores with strong absorption and fluorescence bands in the near-IR (NIR) region due to advances in optical imaging, microarrays, and electrophoresis and the need to develop labels and optical sensors for biological and medical applications.[1] A key advantage of NIR dyes is that the scattering of light, autofluorescence, and absorption by tissues and cells is minimized.[1f,2] Traditionally, cyanine dyes, such as Cy3 or Cy5, have been used for these applications, but poor photostability and low fluorescence quantum yields are often encountered, because rotation and photoisomerization of the flexible structure can result in nonradiative deactivation pathways.[1g,3] There has been increasing interest in the use of boradiazaindacene (BODIPY) dyes for these applications,[4] since they often have superior spectral characteristics to those of fluoresceins and rhodamines. BODIPYs have already started to be used in some contexts.[5]

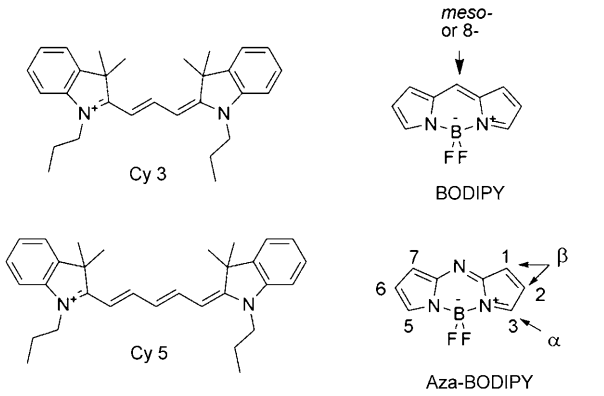

The BODIPY π-system typically absorbs and emits in the 480–540 nm region.[6] Marked red shifts of the absorption and emission maxima have been achieved through aryl or styryl substitution at the 1-, 3-, 5-, and/or 7-positions,[7] aromatic ring fusion,[7h,8] by incorporating an oxygen atom into the π-system to coordinate the boron,[9] or by replacing the *meso*-carbon atom with an aza-nitrogen atom to form an aza-BODIPY.[10] Over the past decade, aza-BODIPY dyes have been studied extensively by the O'Shea research group.[11,14–15] A key advantage of aza-BODIPY dyes is that a marked red shift of the absorption and emission bands relative to conventional BODIPY dyes can be achieved without modifying the key properties of BODIPY dyes, such as their high molar absorption coefficients, narrow and structured absorption and emission bands, small Stokes shifts, high fluorescence quantum yields, and photostability. Two methods have typically been used to prepare aza-BODIPY dyes with 1,3,5,7-tetraaryl substituents,[4b,12] the reaction of a pyrrole with a nitrosopyrrole, which is prepared either in a separate step or in situ, and the formation of aza-dipyrromethene skeletons from chalcones and nitromethane, or cyanide, followed by a condensation reaction with ammonium acetate. Carreira and co-workers recently reported a further bathochromic shift of the lowest-energy absorption band maximum of conventional 1,3,5,7-tetraaryl aza-BODIPY dyes from 688 to 740 nm by restricting the conformational flexibility of the 3- and 5-diaryl moieties by incorporating additional carbocyclic or heterocyclic rings.[10c,12a] However, the synthesis of these compounds requires six steps.

The use of NIR fluorescent aza-BODIPY dyes in practical applications is only likely to become feasible when a facile and commercially viable synthetic method has been developed. Our recently reported novel synthetic method for obtaining benzo-fused aza-BODIPY, **2**, in moderate yield through a two-step reaction of phthalonitrile and an arylmagnesium bromide may provide the solution,[13] since phthalonitrile is commercially available and arylmagnesium

[a] Dr. H. Lu, Prof. Z. Shen
State Key Laboratory of Coordination Chemistry
Nanjing National Laboratory of Microstructures
School of Chemistry and Chemical Engineering
Nanjing University, Nanjing 210093 (China)
Fax: (+86) 25-8331-4502
E-mail: zshen@nju.edu.cn

[b] Dr. H. Lu, Dr. S. Shimizu, Dr. J. Mack, Prof. N. Kobayashi
Department of Chemistry, Graduate School of Science
Tohoku University, Sendai 980–8578 (Japan)
Fax: : (+81) 22-795-7719
E-mail: nagaok@m.tohoku.ac.jp

Supporting information for this article is available on the WWW under http://dx.doi.org/10.1002/asia.201000641.

bromides are easily prepared. A marked red shift of the absorption and emission bands was observed relative to the spectra of conventional 1,3,5,7-tetraaryl aza-BODIPY dyes.[13,14] The introduction of additional substituent groups on the precursors is straightforward, so the spectral properties of the aza-BODIPY product can be readily fine-tuned. This can be problematic with other aza-BODIPY synthetic methods. Phthalonitriles are used industrially during the synthesis of phthalocyanines, so the synthesis and properties of substituted phthalonitriles have already been studied in depth.[15] In this paper, we explore the synthesis of a wider range of 3,5-diaryl aza-BODIPY dyes based on the reaction of arylmagnesium bromides with phthalonitriles and naphthalenedicarbonitriles (Scheme 1). Optical spectroscopy and time-dependent DFT (TD-DFT) calculations are used to investigate the impact of fused-ring-expansion and the introduction of aryl groups with strongly electron-donating dimethylamino substituents at the *para*-positions on the electronic structure and fluorescence properties of the aza-BODIPY chromophore.

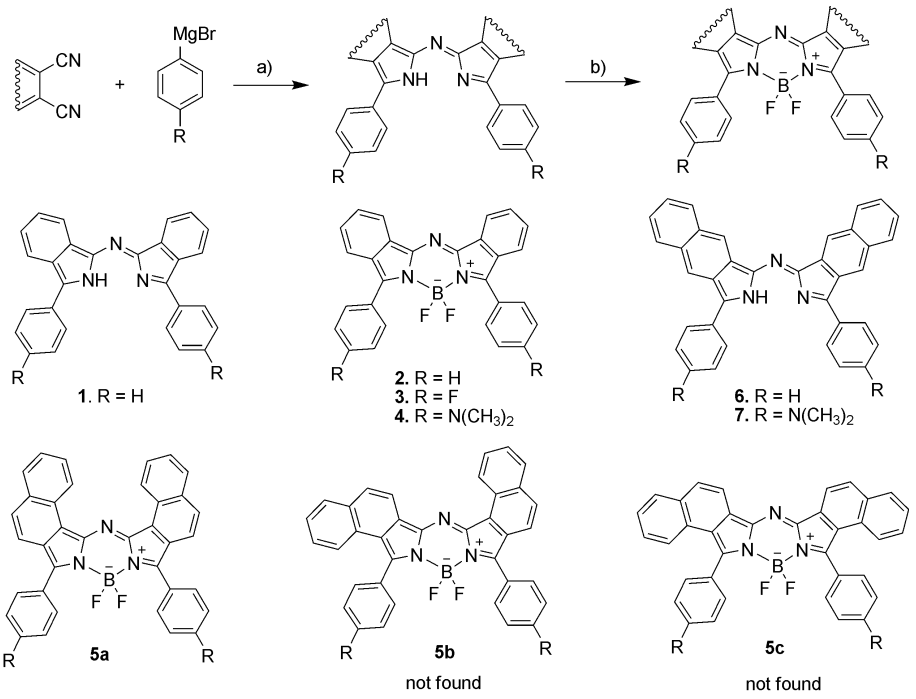

Scheme 1. Synthesis and chemical structures of the aromatic-ring-fused aza-BODIPY and aza-dipyrromethene dyes. a) dry benzene, RT, 1 h; b) BF_3·OEt_2, triethylamine, benzene, reflux.

Results and Discussion

Synthesis

Fused-ring-expanded aza-BODIPYs were prepared by using a method that we have reported previously.[13] Compounds **2**–**4** (Scheme 1) were formed in approximately 24–28% yields by reacting a phthalonitrile (0.1 mol) with an arylmagnesium bromide (0.25 mol) followed by treatment with BF_3·OEt_2. When 1,2-naphthalenedicarbonitrile was used, only one of the three possible 1,2-naphtho-fused aza-BODIPY isomers, **5a**, was formed in 28% yield (Scheme 1). The structure of **5a** was determined based on the ^{1}H NMR spectrum (Figure 1). The assignment of the proton signal is based on the integrated intensities and coupling patterns observed in the H–H COSY NMR spectrum (see the Supporting Information). A doublet signal at very low field (ca. $\delta =$ 9.54 ppm) was assigned to the protons on the naphthalene moiety, which lie closest to the *meso*-nitrogen atom. A similar signal was recently reported in the ^{1}H NMR spectrum of tribenzo[*b*,*g*,*l*]naphtho[1,2-*q*]porphyrazine.[16] Unfortunately, 2,3-naphtho-fused aza-BODIPYs could not be isolated due to instability in solution, but precursors **6** and **7** have been characterized based on MALDI-TOF MS and the presence of characteristic aza-dipyrromethene bands in the UV/Vis absorption spectra (see the Supporting Information, Figure S3).

The use of substituted phthalonitriles provides scope for introducing additional substituent groups, which can be used to further fine-tune the electronic and optical properties of the aza-BODIPY dye. Tetrafluorophthalonitrile and 4,4′-*N*,*N*′-dimethylaminophenyl magnesium bromide were selected as precursors, since aza-BODIPYs containing both electron–donor and acceptor moieties are likely to exhibit novel electron-transfer properties. When the synthesis was carried out, however, the molecular weight of the aza-BODIPY target compound ($[M]^+ = 675$ amu) could not be detected by MALDI-TOF-MS. The main peak was observed instead at m/z: 441, despite the fact that multiple signals observed in the ^{1}H NMR spectrum at $\delta = 8.12$ and 6.77 ppm (m, 4H),

Abstract in Chinese:

通过溴化芳基镁与苯二氰或者萘二氰反应合成了一系列芳环稠合的氮杂硼-二吡咯亚甲基（aza-BODIPY）染料。根据 X-射线结构分析、光谱性质和理论计算对化合物的结构和性质的相关性进行了研究，发现苯并和 1,2-萘并-3,5-二芳基 aza-BODIPY 的吸收和荧光光谱红移进入近红外区域（> 700 nm），这是由于它们的前线分子轨道的能级较 1,3,5,7-四芳基 aza-BODIPY 的能级发生了较大的变化。由于空间位阻效应，我们只得到了三个 1,2-萘并 aza-BODIPY 异构体中的一种分子；由于 2,3-萘并 aza-BODIPY 在溶液中不稳定，无法表征其结构。在苯并-3,5-aza-BODIPY 的对位引入二甲基氨基基团，使得其荧光发生淬灭，在不同的 pH 条件下，溶液的颜色蓝移且荧光增强，可望作为近红外的荧光增强型探针。

CHEMISTRY
AN ASIAN JOURNAL

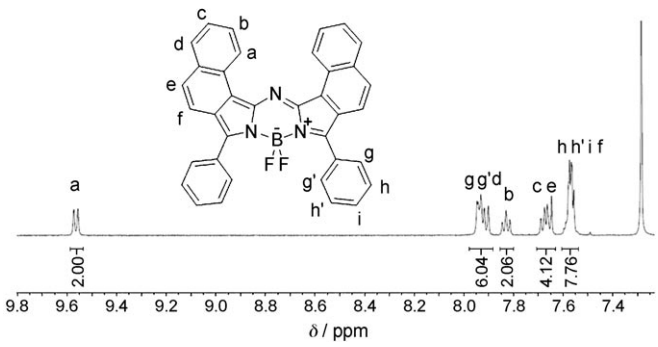

Figure 1. ^{1}H NMR spectrum of **5a** in $CDCl_3$.

along with singlet peaks at $\delta = 3.12$ and 3.09 ppm (s, 6H), are consistent with the presence of two dimethylaminophenyl substituents. X-ray crystallographic analysis revealed that **8** had been obtained (Figure 2).

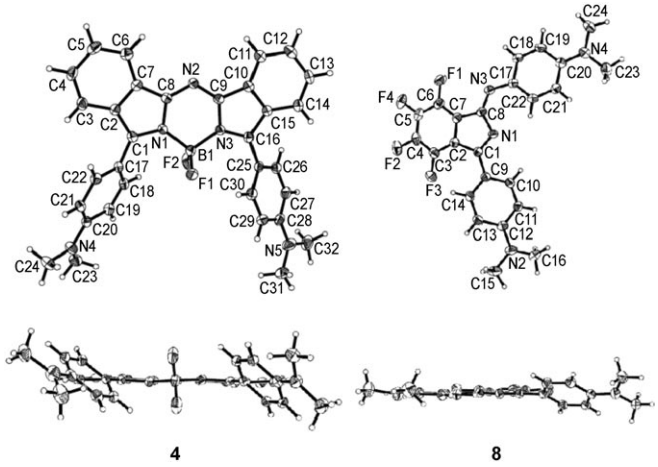

Figure 2. Front (top) and side (bottom) ORTEP views of the molecular structure of **4** and **8** with the thermal ellipsoids set at 50% probability.

The reaction mechanism in Scheme 2 is based on two reactions of phthalonitrile and phenylmagnesium bromide that were previously proposed by other authors.[17] In the 1920s, Weiss and Schlesinger[17a] reported that an unsubstituted version of **8** is obtained in very low yield. Bredereck and Vollmann[17b] later claimed that this was incorrect and that aza-dipyrromethene is instead formed in moderate yield. The X-ray structures of **4** and **8** (Figure 2) provide definitive evidence that both reactions are, in fact, possible. After an initial nucleophilic attack by the Grignard reagent at the carbon atom of the nitrile moiety, magnesium [(2-cyanoaryl)(aryl)methylene]amide bromide (**11**) is formed, which subsequently undergoes ring cyclization to form magnesium (3-aryl-1*H*-isoindol-1-ylidene)amide bromide (**10**). The magnesium salt of **10** reacts with either the aryl magnesium compound to form **8** or with the phthalonitrile to form magnesium (*Z*)-[3-(3-aryl-1*H*-isoindol-1-ylideneamino)-1*H*-isoindol-1-ylidene]amide bromide (**9**), which then reacts with the Grignard reagent to form an aza-dipyrromethene. $BF_3{\cdot}OEt_2$ can be used to convert the aza-dipyrromethene into the aza-BODIPY dye.

X-ray Crystal Structures of 4 and 8

The X-ray crystal structure of **4** is shown in Figure 2. The boron atom is coordinated by two nitrogen atoms (B–N bond lengths of 1.564 and 1.573 Å) and two fluorine atoms (B–F bond lengths of 1.375 and 1.379 Å) in a tetrahedral geometry. The structure is similar to those observed previously in BODIPY structures.[13,14,18] The N4–C20 and N5–C28 bonds (average value: 1.368 Å) are shortened due to conjugation with the lone-pair electrons of the nitrogen atoms in the dimethylamino groups. The indacene moiety has a highly planar structure. The average root-mean-square (rms) deviation of the indacene plane atoms is 0.0452 Å. The dihedral angles between the indacene plane and the phenyl rings at the 3- and 5-positions are 49.5 and 43.4°, respectively (Figure 2). The conjugation properties and the planarity of the π-system play a key role in determining the spectroscopic properties of BODIPYs. The structure of **8** is also planar with an rms value of 0.0307 Å. The dihedral angle between the phenyl ring C9–C14 and the plane of the π-system is 32.5°. The N1–C1 and N3–C8 bond lengths (1.314 and 1.291 Å, respectively) are consistent with double-bond character, in contrast, for instance, with the significantly longer bond lengths (1.405 Å) of N1–C8 and N3–C17 (Figure 2). Head-to-tail π–π stacking interactions are observed in the molecular packing diagrams with interplanar separations of approximately 3.2 Å for **4** and 3.37 Å for **8** (Figure 3).

Optimized Geometries of 5a–c

Although three isomers, **5a–c**, can potentially be formed when 1,2-naphthalenedicarbonitrile is used as the precursor (Scheme 1), only isomer **5a** was isolated and characterized. Steric effects are the most likely explanation for this. B3LYP geometry optimizations were carried out to explore this question. Somewhat surprisingly, the indacene plane of **5a** is predicted to be near planar (Figure 4), despite the fact that the outer benzene rings of the 2,3-naphthalene moieties are aligned towards each other. The absence of a *meso*-substituent in the aza-BODIPY structure reduces the scope for steric crowding. In the structures of **5b** and **5c**, interatomic distances of approximately 2.63 Å are predicted between hydrogen atoms of the peripheral 1,2-naphtho-fused ring moieties and carbon atoms of the phenyl substituents (Figure 4). This is considerably shorter than the sum of the van der Waals radii for the carbon and hydrogen atoms of benzene, 2.77 Å.[19] It seems probable, therefore, that there is a much higher energy barrier to the formation of **5b** and **5c**.

Absorption and Fluorescence Spectroscopy

The main absorption band of **2** in dichloromethane lies at 712 nm and the corresponding fluorescence band lies at

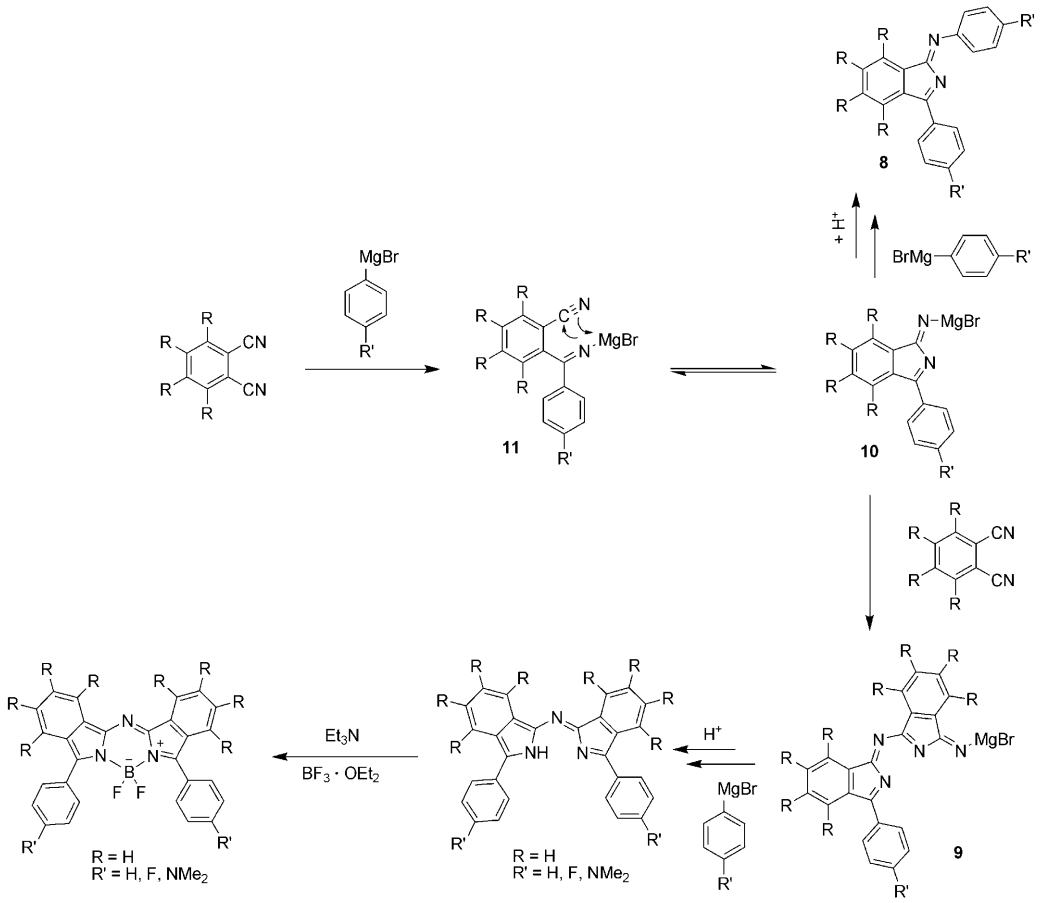

Scheme 2. Reaction mechanisms for the formation of aza-BODIPY and **8**.

736 nm. Fused-ring-expansion with benzene rings results in a 62 nm red shift of the absorption band relative to that of 1,3,5,7-tetraaryl aza-BODIPYs ($\lambda_{max} \approx 650$ nm).[14] Smaller extinction coefficients are observed in the spectrum of **3** when electron-withdrawing fluorine substituents are added at the *para*-positions, but the other spectroscopic properties, such as the absorption and fluorescence band maxima and the quantum yield remain almost unchanged. When two dimethylamino substituents are present at the *para*-positions of the phenyl rings in **4**, the absorption peak at 794 nm becomes significantly broader than those observed in the spectrum of **2**. A significant red shift of 82 nm is observed for the band center of the lowest-energy absorption band in dichloromethane. Slight red shifts of 25 and 17 nm are observed in the absorption and emission bands of the 1,2-naphtho-fused compound, **5a**, along with small changes in the full width at half maximum (fwhm), Stokes shift, and fluorescence quantum yield values.

Three solvents with markedly differing polarities were selected to carry out an in depth investigation of the photophysical properties of **2**–**5a**. For **2**, **3**, and **5a**, the fwhm of the lowest-energy absorption bands increases slightly as a function of solvent polarity (Table 1), probably due to the high rigidity and weak dipolar nature of the chromophores.[20] In contrast, the fwhm of **4** changes markedly due to the relatively large ground-state dipole moment of 6.39 D. The integrated intensity of the lowest-energy absorption band remains constant regardless of any change in the solvent polarity (Figure 5).

The fluorescence spectra typically exhibit mirror symmetry with the absorption bands. The lack of a clear trend in the emission band centers of **2**, **3**, and **5a** is consistent with emission from the relaxed Franck–Condon excited state.[8c] The absorbance band centers and Stokes shifts of **2** and **3** are relatively insensitive to solvent effects with only a minor blue shift observed at high solvent polarity in acetonitrile relative to nonpolar hexane solutions. However, the fluorescence quantum yield and Stokes shift of **4** exhibit a marked solvent dependence. The fluorescence quantum yield of **4** is 0.10 in hexane, but only 0.01 in dichloromethane and acetonitrile. Quenching of fluorescence intensity in polar solvents is often attributed to an intramolecular charge-transfer process[18,21,22] and may be related to efficient nonradiative relaxation caused by conical intersections formed between the potential-energy surfaces of close-lying excited states of the same multiplicity.[23]

CHEMISTRY
AN ASIAN JOURNAL

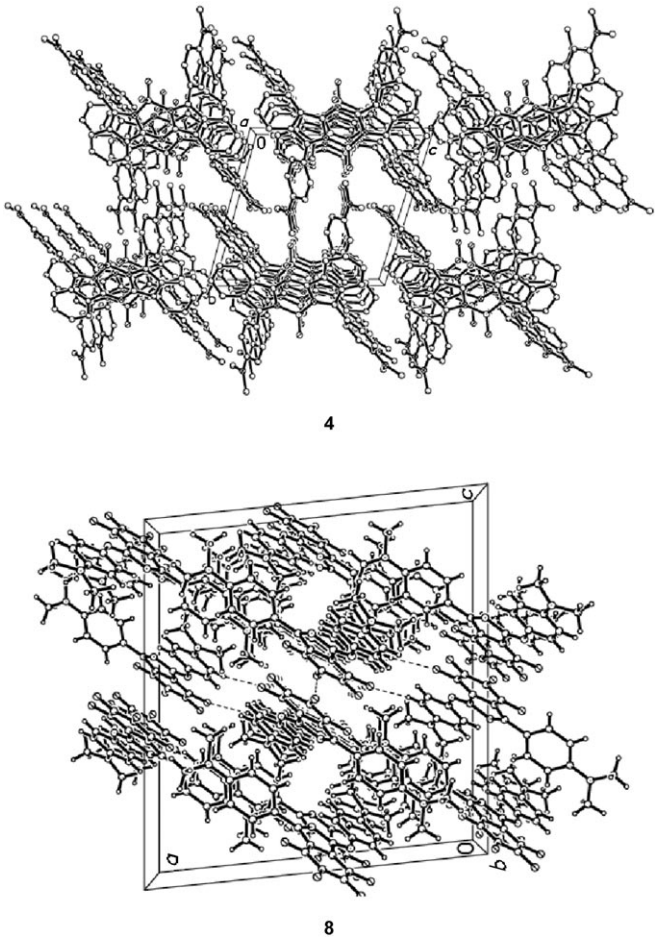

Figure 3. Molecular packing in the crystal structures of **4** and **8** viewed along the *a*-axis.

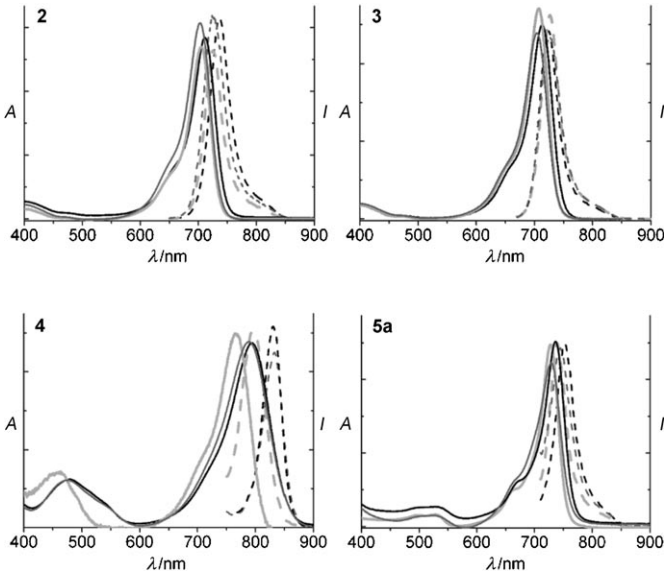

Figure 5. Absorption and fluorescence spectra of **2**–**5a** in dichloromethane (——), hexane (——), and acetonitrile (——).

Molecular Orbits and Transition

TD-DFT calculations were carried out to derive an enhanced understanding of the observed spectroscopic properties of **2**–**5a** (see the Supporting Information). Figure 6 contains a partial MO energy diagram for the frontier π-MOs at the B3LYP/6-31G(d) level of theory. The lowest-energy excitation of **4** is predicted to lie at 655 nm ($f=0.79$) and to arise primarily from the HOMO→LUMO one-electron transition (Table 2). The HOMO and LUMO of **4** are both destabilized relative to those of **2** due to the strong electron-donating properties of the dimethylamino substituents. There is a marked red shift of the absorption and emission bands of **4**, as the destabilization of the HOMO is greater

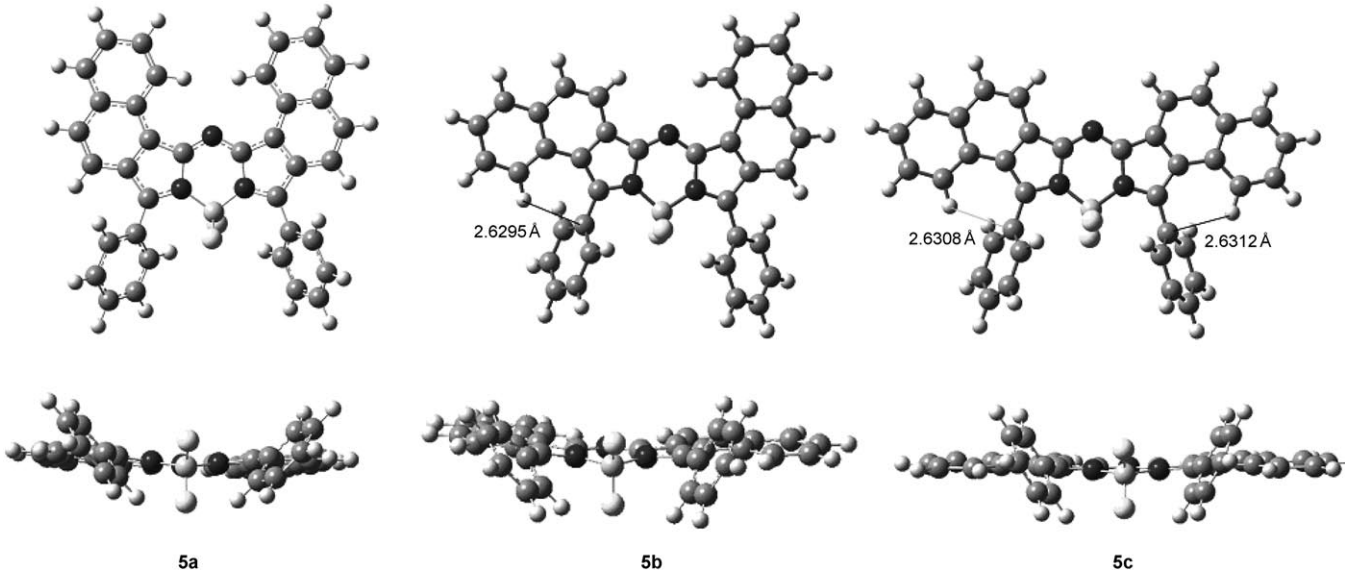

Figure 4. B3LYP-optimized geometries of the three 1,2-naphtho-fused isomers **5a**, **5b**, and **5c** calculated with the 6-31G(d) basis set.

Table 1. Spectroscopic data of **2**–**5a** in hexane, dichloromethane, and acetonitrile at 298 K.

Dye	Solvent	λ_{abs} [nm]	fwhm [nm]	ε [$M^{-1}cm^{-1}$]	λ_{em} [nm]	Stokes shift [nm]	Φ_f
2	hexane	705	43	n.d.[a]	725	20	0.24
	CH_2Cl_2	712	47	95000	736	24	0.14
	MeCN	704	48	51000	725	21	0.20
3	hexane	707	41	n.d.[a]	726	19	0.17
	CH_2Cl_2	713	46	63000	724	11	0.16
	MeCN	702	48	44000	726	24	0.19
4	hexane	765	63	n.d.[a]	796	31	0.10
	CH_2Cl_2	794	82	174000	830	36	0.01
	MeCN	789	90	91000	833	45	0.01
5a	hexane	728	37	n.d.[a]	739	11	0.30
	CH_2Cl_2	737	43	71000	753	16	0.14
	MeCN	729	58	35800	745	16	0.20

[a] Not determined due to low solubility.

than that of the LUMO. The wavelengths and intensities of the second to fourth lowest-energy transitions in the calculated spectrum closely match the experimental data in the 430—580 nm region (Table 2 and the Supporting Information, Figure S2). The lowest energy band of the 1,2-naphtho-fused compound, **5a**, shifts to longer wavelength by approximately 25 nm (Figure 5). The HOMO and LUMO of **5a** are almost fully localized on the aza-BODIPY core and have nodal patterns, which are very similar to those of the frontier MOs of **2** (Figure 6). The HOMO–LUMO energy gap is almost unchanged and the red shifts of the absorption and emission bands closely match the trends predicted in the theoretical calculations. The lowest-energy transition of **3** is predicted to lie at 595 nm ($f=0.75$) well to the blue of the corresponding band of **4** due to the effect of the electron-withdrawing substituents on the energies of the frontier MOs. The broader and weaker absorption band of **5a** in the 500—550 nm range can be assigned to the second and third lowest-energy transitions, which are predicted to lie at 505 and 502 nm ($f=0.02$, 0.16), and to arise primarily from the HOMO–1→LUMO and HOMO–2→LUMO transitions, respectively (Table 2 and the Supporting Information).

Additional theoretical calculations were carried out for 3,5-diaryl-aza-BODIPY (**12**) and the corresponding 2,3-naphtho-fused aza-BODIPY compound (**13**) so that the effect of fused-ring expansion could

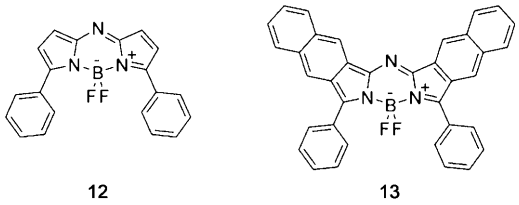

12 13

be explored (Table 3). A consistent red shift of the $S_0 \rightarrow S_1$ band is observed as each additional pair of benzene rings is added to the π-system. Since the core of the aza-BODIPY structure forms part of the π-system of tetraazaporphyrins

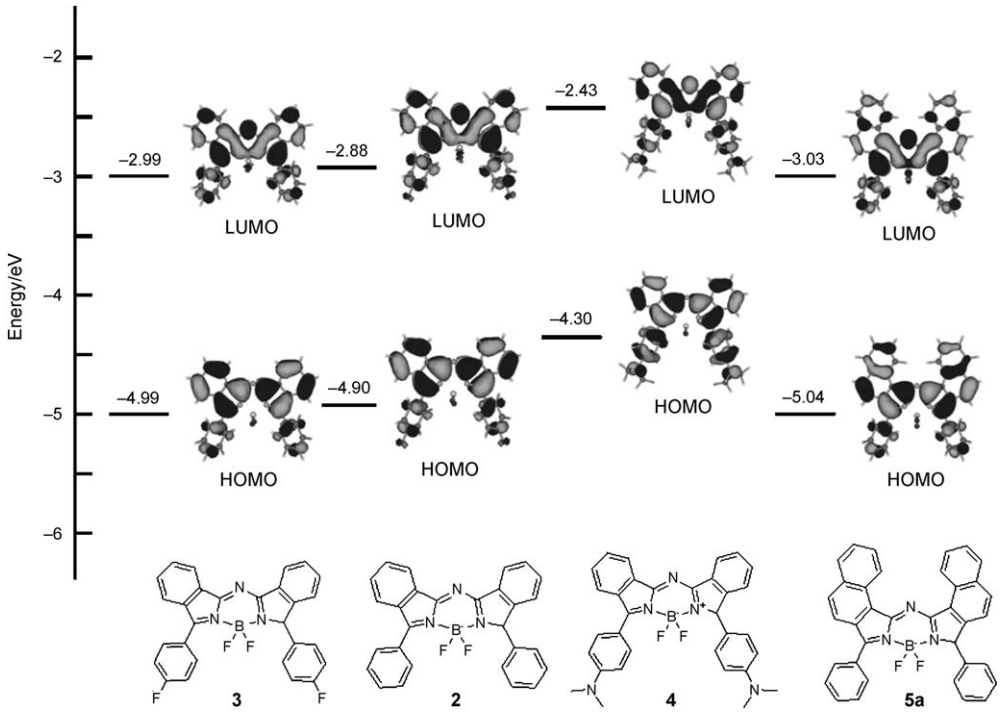

Figure 6. Energy-level diagram for the frontier π-MOs of dyes **2**–**5a**. Nodal patterns of each MO are shown at an isosurface value of 0.02.

CHEMISTRY
AN ASIAN JOURNAL

Table 2. Calculated electronic excitations energies, oscillator strengths, and the related wave functions.

Dye	Energy [eV]	λ [nm]	f[a]	Wave function[b]
2	2.10	590	0.75	62% |L←H>
3	2.08	595	0.75	62% |L←H>
4	1.89	655	0.79	64% |L←H>, 1% |L←H-2>
	2.61	476	0.22	88% |L←H-1>, 5% |L+1←H>
	2.79	444	0.02	88% |L←H-2>
	3.18	390	0.25	82% |L+1←H>, 1% |L←H-1>, 2% |L←H-4>
5a	1.98	627	0.60	64% |L←H>, 5% |L←H-2>
	2.46	505	0.02	92% |L←H-1>
	2.47	502	0.16	88% |L←H-2>, 1% |L←H>

[a] Oscillator strength. [b] The wave functions based on the eigenvectors predicted by TD-DFT.

(also known as porphyrazines), a comparison can also be made with the Q bands of the corresponding porphyrazine (Pz), phthalocyanine (Pc), and 1,2- and 2,3-naphthalocyanine (1,2-Nc and 2,3-Nc) compounds (Table 3).[16b] A similar consistent red shift of the $S_0 \rightarrow S_1$ band is observed. Although greater variation is observed in the calculated oscillator strengths of the fused-ring-expanded porphyrazines, due to the orbital angular momentum properties of the cyclic heteroaromatic tetrapyrrole structure,[24] it seems reasonable to conclude that trends observed in the wavelengths of fused-ring-expanded porphyrazines can be used as a guide to determine the optical properties of the corresponding aza-BODIPY. Since a very wide range of fused-ring-expanded porphyrazines have been characterized,[25] this should greatly facilitate the selection of phthalonitriles required to synthesize aza-BODIPYs with properties suitable for use in specific practical applications.

Detailed insights have also been derived on the electronic structures and optical spectroscopy of 2,3-naphtho-fused dipyrromethene intermediates **6** and **7**. Comparison with experimental data is problematic in the context of **7**, since it is very unstable and decomposes almost immediately in solution.

The HOMOs of **6** and **7** are delocalized over the entire indacene plane, unlike that of **5a** (Figure 6 and 7). The energies of the HOMO and LUMO of **6** are destabilized relative to the frontier MOs of **1**. The same trend is also observed in calculations carried out for **2** and the corresponding aza-BODIPY compounds (BF_2-**6** and BF_2-**7**). It seems safe to conclude that BF_2-**6** and BF_2-**7** are easily oxidized by oxygen in solution and this accounts for why they are too unstable to be isolated and characterized. A large red shift from 650 to 754 nm is observed for the lowest-energy absorption band of BF_2-**6** relative to **2** (see the Supporting Information, Figure S4), since the destabilization of the HOMO is greater than that of the LUMO, thus resulting in narrowing of the HOMO–LUMO band gap ($\Delta E = 2.13$ for **1**, 1.82 eV for **6**). The lowest-energy band is consistently predicted to arise from the HOMO→LUMO transition (Table 2 and the Supporting Information, Table S4). A further red shift from 754 to 806 nm is observed in the spectrum of **7** relative to that of **6** due to the presence of the dimethylamino substituents (see the Supporting Information, Figure S3). A further slight narrowing of the HOMO–LUMO band gap ($\Delta E = 1.78$ eV for **7**) is predicted in the TD-DFT cal-

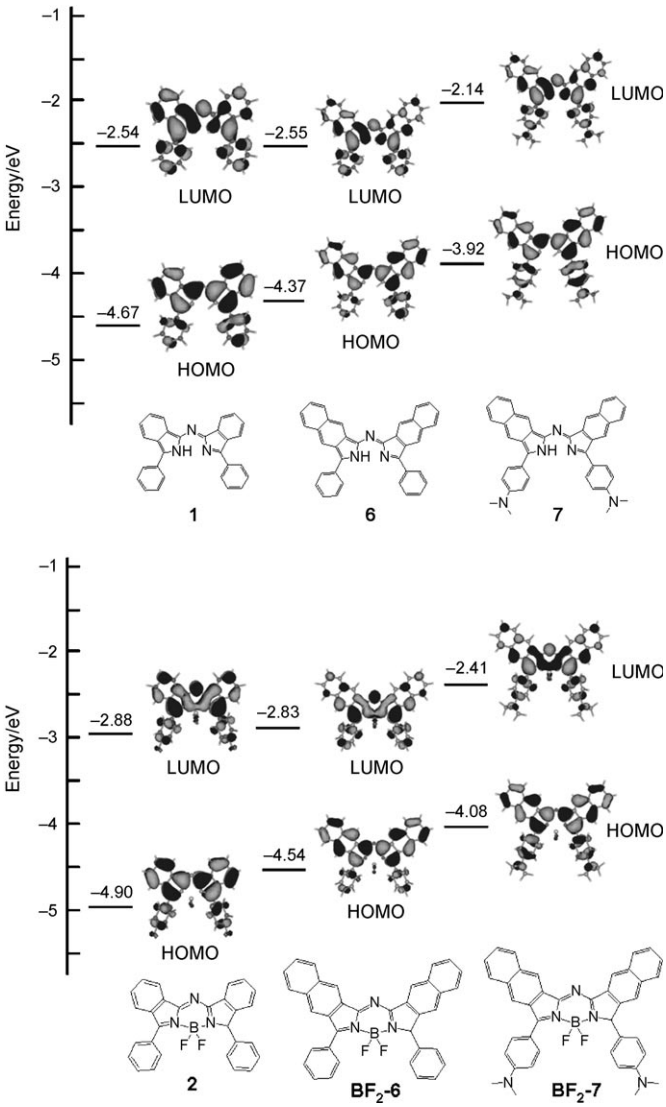

Figure 7. Energy-level diagram for the frontier π-MOs of dyes **1**, **6**, and **7** (top) and the corresponding BODIPY complexes (bottom). Nodal patterns of each MO are shown at an isosurface value of 0.02.

Table 3. Calculated wavelengths (λ_{calcd}), intensities, and the observed wavelengths (λ_{obs}) of the $S_0 \rightarrow S_1$ transitions of fused-ring-expanded aza-BODIPYs and porphyrazines.

Fused ring	BODIPY	λ_{calcd} [nm]	f[a]	λ_{obs} [nm]	ZnPz[b]	λ_{calcd} [nm]	f[a]	λ_{obs} [nm]
–	**12**	517	0.69	n.a.[c]	Pz	500	0.14	586
benzo	**2**	590	0.75	712	Pc	593	0.40	672
1,2-naphtho	**5a**	627	0.6	737	1,2-Nc	n.a.	n.a.	n.a.
2,3-naphtho	**13**	706	0.74	n.a.	2,3-Nc	695	0.59	756

[a] Oscillator strength. [b] Fused-ring-expanded zinc porphyrazine compounds. [c] n.a. = not available.

culation (Figure 7). The same trends in the HOMO energies, HOMO–LUMO band gaps, and the wavelengths of the lowest-energy bands are also predicted for **2**, BF_2-**6**, and BF_2-**7** (Figure 7 and Table 2 and the Supporting Information, Figure S5 and Table S4).

Electrochemistry

The electrochemical properties of the aza-BODIPYs were studied by cyclic voltammetry in dichloromethane with 0.1 M tetra-*n*-butylammonium perchlorate (TBAP) as a supporting electrolyte. The effects of the replacement of the *meso*-carbon atom with a nitrogen atom and fused-ring expansion of the π-conjugation system can be assessed by comparing the redox potentials for **3**, **5a**, and the corresponding conventional alkyl-substituted BODIPY compound (Figure 8). In our previous studies of BODIPYs, an extension of the π-conjugation system of the indacene chromophore through fusion with benzene rings at β-pyrrole positions caused a significant destabilization of the HOMO energy level, while the LUMO energy level is only slightly destabilized. For example, the reduction and oxidation potentials of the conventional alkyl-substituted BODIPY were observed at −1560 and 760 mV (vs. ferrocenium/ferrocene (Fc^+/Fc)), respectively, while those of the benzo-fused BODIPY lie at −1530 and 330 mV (vs. Fc^+/Fc), respectively.[8c]

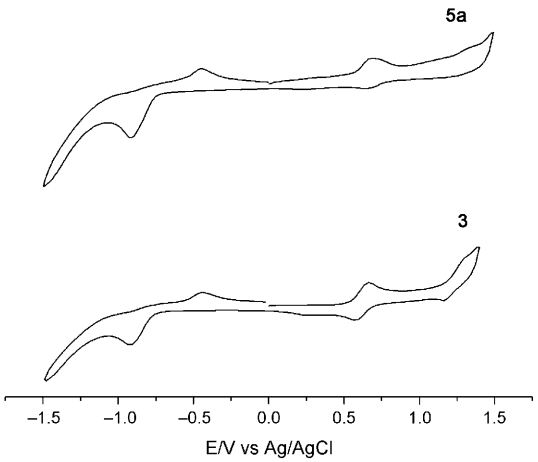

Figure 8. The CV scans of **3** and **5a**.

The cyclic voltammogram of aza-BODIPY **3** contains an irreversible one-electron reduction step at −610 mV and a reversible oxidation step at 460 mV (vs. Fc^+/Fc). The first reduction potential is substantially lower than that of alkyl-substituted BODIPYs, as the incorporation of the electronegative nitrogen atom at the *meso*-carbon position causes a marked stabilization of the LUMO. In DFT calculations, a large MO coefficient is predicted at the *meso*-carbon position in the LUMO, while, in contrast, this atom lies on a nodal plane of the HOMO (Figure 6). The stabilization of the LUMO leads to narrowing of the HOMO–LUMO band gap and hence results in the marked red shift of the lowest-energy absorption bands observed for aza-BODIPYs relative to those of the corresponding BODIPY dyes. When the π-conjugation system is extended to form the 1,2-naphtho-fused aza-BODIPY **5a**, only minor changes are observed in the first oxidation and reduction steps as would be anticipated based on the small changes observed in the HOMO and LUMO energies (Figure 6 and 8). A significant decrease in the first oxidation potential would be expected if a 2,3-naphtho-fused aza-BODIPY could be successfully synthesized, due to the marked destabilization predicted for the HOMO (Figure 7).

pH-Dependent Absorption and Fluorescence Spectroscopy of 4

O'Shea et al. recently reported a dimethylamino-substituted 1,3,5,7-tetraaryl aza-BODIPY with pH-dependent colorimetric and fluorescent "turn-on" responses.[11b] Two protonation steps were observed during titration with trifluoroacetic acid (TFA). The pH dependence of the absorption and fluorescence bands of the corresponding benzo-fused 3,5-diaryl aza-BODIPY was analyzed based on the sequential addition of TFA to a dichloromethane solution of **4**. Upon addition of TFA, a stepwise blue shift of the 794 nm band is observed along with a slight decrease of the extinction coefficient (Figure 9). Further addition of TFA results

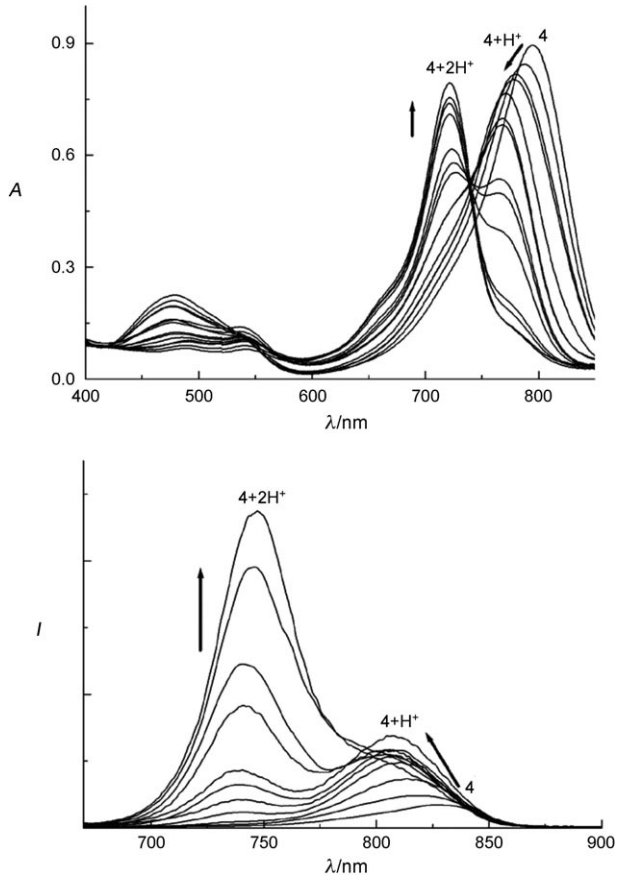

Figure 9. Absorption and fluorescence (λ_{ex} = 650 nm) spectra of **4** in dichloromethane titrated with TFA.

in a decrease in the intensity of the 771 nm band of **4**-H^+ and a new blue shifted absorption band at 724 nm. The presence of an isosbestic point at 740 nm is consistent with the quantitative formation of a diprotonated **4**-$2H^+$ species. The emission band of **4** gradually increases in intensity and is shifted to the blue after the addition of TFA because the electron-donating properties of dimethylamino substituents are eliminated upon protonation. Emission intensity increases because the absorption intensity increases at the excitation wavelength due to the spectral changes, which occur when less electron density is accepted by the aza-BODIPY chromophore. As the concentration of TFA is increased, the formation of the **4**-$2H^+$ species results in an additional markedly blue shifted band at 745 nm, which gradually increases in intensity to 15 times that of the lowest-energy absorption band of **4** (Figure 8). The absorption and fluorescence spectra of **4**-$2H^+$ are similar to those of **2**, which contains unfunctionalized phenyl rings. The TFA titration spectra reveal that **4** can be used as a ratiometric "turn-on" fluorescence sensor for changes in pH and that NIR dyes with ratiometric "turn-on" response can be designed rationally by introducing electron-donating substituents at the *para*-position of the phenyl rings of fused-ring-expanded aza-BODIPYs.

Conclusions

The synthesis, characterization, and theoretical analysis of a series of fused-ring-expanded aza-BODIPY NIR dyes have been described. The use of phthalonitriles and arylmagnesium bromides as precursors is clearly very promising and could eventually provide a facile method for bulk synthesis, which will facilitate the use of aza-BODIPYs in practical applications, but challenges remain. 2,3-Naphtho-fused aza-BODIPY was found to be unstable in solution, while aza-BODIPY was only obtained as a trace level product when fluoro- and dimethylamino substituents were introduced on the phthalonitrile and arylmagnesium bromide precursors, due to the formation of an isoindoline compound, **8**. Further studies are underway to investigate in depth which types of substituted phthalonitriles and naphthalenedicarbonitriles can be used to form aza-BODIPYs as the major product. Benzo- and 1,2-naphtho-fused aza-BODIPYs and 2,3-naphtho-fused compounds exhibit modified spectroscopic properties due to changes to the energies of the frontier MOs, but the high molar absorptivity of the lowest energy $S_0 \rightarrow S_1$ band and the key fluorescence properties of BODIPY are retained. The red shift observed in the wavelength of the $S_0 \rightarrow S_1$ absorption band parallels that observed for the Q band of the corresponding phthalocyanine and naphthalocyanine complexes.[16b] This suggests that it may be possible to make use of trends observed in the properties of NIR absorbing phthalocyanines as a guide to enable the rational design of aza-BODIPY structures with properties suitable for specific practical applications. When an electron-donating dimethylamino group is introduced at the *para*-position of the arylmagnesium precursor, there is an intensification and red shift of the lowest energy aza-BODIPY absorption band from 712 to 794 nm in dichloromethane and a quenching of the fluorescence in polar solvents. These processes can be utilized to provide a ratiometric "turn-on" probe for changes in pH, based on the effect of protonation at the dimethylamino groups. Attempts to design and synthesize aza-BODIPYs suitable for use in aqueous media are currently underway.

Experimental Section

General: All reagents were obtained from commercial suppliers and used without further purification unless otherwise indicated. All air and moisture-sensitive reactions were carried out under a nitrogen atmosphere. Triethylamine was obtained by simple distillation. The ^{1}H NMR spectroscopic measurements were made by using a Bruker 500 MHz spectrometer and a JEOL GSX-400 spectrometer with $CDCl_3$ as the solvent. Mass spectra were recorded on Perspective Biosystem MALDI-TOF MassVoyager DCE-S12 and Micromass LCT ESI-TOF MS spectrometers. HRMS were recorded on a Bruker Daltonics Apex-III spectrometer. Fluorescence spectral measurements were carried out by using a Hitachi F-4500 spectrofluorometer. Electronic absorption spectra were recorded with Hitachi U-3410 and JASCO V-570 spectrophotometers. Quantum yields were determined relative to magnesium phthalocyanine ($\Phi_F = 0.84$, upon excitation at 630 nm).[26] Selected redox properties were studied by cyclic voltammetry in TBAP (0.1 M) in acetonitrile on a Perkin–Elmer electrochemical analysis system model 283 with a platinum disk as the working electrode, Ag/AgCl as the quasi-reference electrode, and a platinum wire as the counter-electrode. Redox potentials were referenced internally against Fc^+/Fc. All measurements were performed under an inert atmosphere with a scan rate of 100 mVs^{-1} at room temperature.

Synthesis: The general procedure for the preparation of dyes **2**–**5a** is to first vigorously stir phthalonitrile (100 mmol) in a dry benzene solution (40 mL). A diethyl ether or tetrahydrofuran solution (THF; 40 mL) of the relevant Grignard reagent (0.25 mol) is then added at room temperature and the resulting mixture is stirred for a further 1 h. The flask is then cooled to 0–5 °C and the excess of the Grignard reagent is decomposed carefully with 20% ammonium chloride. The solvent is removed by using a rotary evaporator and the residue distilled with water steam, filtered, dried, and subsequently treated with $BF_3{\cdot}OEt_2$ in the presence of triethylamine in refluxing benzene. Column chromatography was used to purify **2**–**5a**, followed by recrystallization from CH_2Cl_2/hexane. The melting point of each compound exceeds 200 °C.

Compound 3: Compound **3** was prepared from phthalonitrile and 4-fluorophenylmagnesium bromide in 24% yield under similar reaction conditions and was treated with $BF_3{\cdot}OEt_2$ in the presence of triethylamine in refluxing benzene. UV/Vis (CH_2Cl_2): λ_{max} (ε) = 713 nm (63000); ^{1}H NMR (400 MHz, $CDCl_3$, 297 K): $\delta = 8.12$ (d, $J = 8$ Hz, 2H), 7.89 (m, 4H), 7.61 (d, $J = 8.4$ Hz, 2H), 7.53 (m, 4H), 7.49 (dd, $J_1 = 8.8$, $J_2 = 5.2$ Hz, 2H), 7.29 ppm (m 2H); MALDL-MS m/z: 481.297; HRMS-ESI: m/z: calcd for $C_{28}H_{16}BF_4N_3Na^+$: 504.1266 $[M+Na]^+$; found: 504.1264.

Compound 4: Compound **4** was prepared in 25% yield from phthalonitrile and 4,4′-*N*,*N*′-dimethyl-aminophenylmagnesium bromide in a similar manner. UV/Vis (CH_2Cl_2): λ_{max} (ε) = 794 nm (174000); MALDL-MS m/z: 531.272; HRMS-ESI: m/z: calcd for $C_{32}H_{28}BF_2N_5Na^+$: 554.2298 $[M+Na]^+$; found: 554.2301.

Compound 5a: Compound **5a** was prepared in 28% yield from 1,2-naphthalenedicarbonitrile in a similar manner. UV/Vis (CH_2Cl_2): λ_{max} (ε) = 737 nm (71000); ^{1}H NMR (500 MHz, $CDCl_3$, 297 K): $\delta = 9.54$ (d, $J = 8.4$ Hz, 2H), 7.91 (m, 6H), 7.80 (m, 2H), 7.64 (m, 4H), 7.54 ppm (m 8H); MALDI-TOF-MS m/z: 545.367; HRMS-ESI: m/z: calcd for $C_{36}H_{22}BF_2N_3Na^+$: 568.1767 $[M+Na]^+$; found: 568.1769.

Compounds 6 and 7: Compounds **6** and **7** were prepared from 2,3-naphthalenedicarbonitrile with phenylmagnesium bromide and 4,4′-*N*,*N*′-di-

methyl-aminophenylmagnesium bromide, respectively. MALDI-TOF-MS m/z: 496.43 for **6**, 583.396 for **7**.

Compound 8: Compound **8** was prepared from 3,4,5,6-tetrafluorophthalonitrile with 4,4′-*N*,*N*′- dimethyl-aminophenylmagnesium bromide and was purified by water steam distillation and column chromatography. ^{1}H NMR (400 MHz, $CDCl_3$, 297 K): $\delta = 8.12$ (m, 4H), 6.77 (m, 4H), 3.12 (s, 6H), 3.09 ppm (s, 6H); MALDI-TOF-MS m/z: 441; HRMS-ESI: m/z: calcd for $C_{24}H_{20}F_4N_4Na^+$: 463.1516 $[M+Na]^+$, $C_{24}H_{20}F_4N_4H^+$: 441.1697 $[M+H]^+$; found: 463.1521, 441.1693.

X-ray structure determination: Data collection for **4** and **8** was carried out at −100 °C on a Rigaku Saturn CCD spectrometer with graphite-monochromatized $Mo_{K\alpha}$ radiation ($\lambda = 0.71070$ Å). The structure was solved by direct methods (SHELXS-97)[27] and refined by using a full-matrix least-square technique (SHELXL-97).[27] Yadokari-XG software was used as a GUI for SHELXL-97.[28]

CCDC-774743 and -774744 contain the supplementary crystallographic data for this paper. These data can be obtained free of charge from The Cambridge Crystallographic Data Centre via www.ccdc.cam.ac.uk/data_request/cif.

Computational details: The G03W software package[29] was used to carry out gas-phase DFT geometry optimizations. The hybrid B3LYP functional was selected and 6-31G(d) basis sets were used. The same approach was used to obtain excitation energies and oscillator strengths from TD-DFT calculations.

Acknowledgements

Financial support was provided by the National Natural Science Foundation of China (nos. 20971066 and 21021062), the Chinese Ministry of Education's Program for New Century Excellent Talents in Universities (no.NCET-08–0272), the Major State Basic Research Development Program of China (grant nos. 2011CB808704 and 2007CB925103), and a Grant-in-Aid for Scientific Research on Innovative Areas (no. 20108007, "pi-Space") from the Japanese Ministry of Education, Culture, Sports, Science, and Technology (MEXT).

[1] a) R. P. Haugland, *Handbook of Fluorescent Probes and Research Products*, *9th ed.*, Molecular Probes, Eugene, OR, **2002**; b) E. U. Akkaya in *Chemosensors of Ion and Molecule Recognition* (Eds.: J.-P. Desvergne, A. W. Czarnik), Kluwer Academic, Dordrecht, **1997**, pp. 177–188; c) E. Terpetschnig, O. S. Wolfbeis in *Near-Infrared Dyes for High Technology Applications* (Eds.: S. Dihne, U. Resch-Genger, O. S. Wolfbeis), Kluwer Academic, Dordrecht, **1998**, pp. 161–182; d) V. Ntziachristos, C. Bremer, R. Weissleder, *Eur. J. Radiol.* **2003**, *13*, 195–208; e) E. M. Sevick-Muraca, J. P. Houston, M. Gurfinkel, *Curr. Opin. Chem. Biol.* **2002**, *6*, 642–650; f) A. Becker, C. Hessenius, K. Licha, B. Ebert, U. Sukowski, W. Semmler, B. Wiedenmann, C. Grötzinger, *Nat. Biotechnol.* **2001**, *19*, 327–331; g) B. Ballou, L. A. Ernst, A. S. Waggoner, *Curr. Med. Chem.* **2005**, *12*, 795–805.

[2] a) G. M. Fischer, M. Isomäki-Krondahl, I. Götker-Schnetmann, E. Daltrozzo, A. Zumbusch, *Chem. Eur. J.* **2009**, *15*, 4857–4864; b) J. V. Frangioni, *Curr. Opin. Chem. Biol.* **2003**, *7*, 626–634; c) C. L. Amiot, S. Xu , S. Liang, L. Pan, J. Xiao, J. Zhao, *Sensors* **2008**, *8*, 3082–3105; d) Z. Cheng, Z. Wu, Z. Xiong, S. S. Gambhir, X. Chen, *Bioconjugate Chem.* **2005**, *16*, 1433–1441; e) R. Weissleder, *Nat. Biotechnol.* **2001**, *19*, 316–317; f) V. Ntziachristos, J. Ripoll, L. H. V. Wang, R. Weissleder, *Nat. Biotechnol.* **2005**, *23*, 313–320; g) E. M. Sevick-Muraca, J. P. Houston, M. Gurfinkel, *Curr. Opin. Chem. Biol.* **2002**, *6*, 642–650.

[3] a) N. Tyutyulkov, J. Fabian, A. Mehlhorn, F. Dietz, A. Tadjer, *Polymethine Dyes*, St. Kliment Ohridski University Press, Sofia, **1991**, pp. 128–137.

[4] a) A. B. Descalzo, H. J. Xu, Z. Shen, K. Rurack, *Ann. N. Y. Acad. Sci.* **2008**, *1130*, 164–171; b) A. Loudet, K. Burgess, *Chem. Rev.* **2007**, *107*, 4891–4932; c) E. Kim, S. B. Park, *Chem. Asian J.* **2009**, *4*, 1646–1658.

[5] a) R. E. Pagano, O. C. Martin, H. C. Kang, R. P. Haugland, *J. Cell Biol.* **1991**, *113*, 1267–1279; b) J. Karolin, L. B.-Q. Johansson, L. Strandberg, T. Ny, *J. Am. Chem. Soc.* **1994**, *116*, 7801–7806; c) T. G. Pavlopoulos, *Prog. Quantum Electron.* **2002**, *26*, 193–224; d) G. Ulrich, R. Ziessel, A. Harriman, *Angew. Chem.* **2008**, *120*, 1202; *Angew. Chem. Int. Ed.* **2008**, *47*, 1184–1201.

[6] a) H. Lu, L. Xiong, H. Liu, M. Yu, Z. Shen, F. Li, X. You, *Org. Biomol. Chem.* **2009**, *7*, 2554–2558; b) Y. H. Yu, Z. Shen, H. Y. Xu, Y. W. Wang, T. Okujima, N. Ono, Y. Z. Li and X. Z. You, *J. Mol. Struct.* **2007**, *827*, 130–136; c) H. Lu, S. S. Zhang, H. Z. Liu, Y. W. Wang, Z. Shen, C. G. Liu, X. Z. You, *J. Phys. Chem. A* **2009**, *113*, 14081–14086; d) R. Ziessel, C. Goze, G. Ulrich, M. Césario, P. Retailleau, A. Harriman, J. P. Rostron, *Chem. Eur. J.* **2005**, *11*, 7366–7378; e) C. W. Wan, A. Burghart, J. Chen, F. Bergström, L. B.-Å. Johansson, M. F. Wolford, T. GyumKim, M. R. Topp, R. M. Hochstrasser, K. Burgess, *Chem. Eur. J.* **2003**, *9*, 4430–4441; f) A. Harriman, L. Mallon, R. Ziessel, *Chem. Eur. J.* **2008**, *14*, 11461–11473; g) H. Lu, Z. L. Xue, J. Mack, Z. Shen, X. Z. You, N. Kobayashi, *Chem. Commun.* **2010**, *46*, 3565–3567.

[7] a) R. Guliyev, A. Coskun, E. U. Akkaya, *J. Am. Chem. Soc.* **2009**, *131*, 9007–9013; b) Y. H. Yu, A. B. Descalzo, Z. Shen, H. Röhr, Q. Liu, Y. W. Wang, M. Spieles, Y. Z. Li, K. Rurack, X. Z. You, *Chem. Asian J.* **2006**, *1*, 176–187; c) K. Rurack, M. Kollmannsberger, J. Daub, *Angew. Chem.* **2001**, *113*, 396–399; *Angew. Chem. Int. Ed.* **2001**, *40*, 385–387; d) K. Rurack, M. Kollmannsberger, J. Daub, *New J. Chem.* **2001**, *25*, 289–292; e) M. Bröring, R. Krüger, S. Link, C. Kleeberg, S, Köler, X. Xie, B. Ventura, L. Flamigni, *Chem. Eur. J.* **2008**, *14*, 2976–2983; f) Q. Zheng, G. Xu, P. N. Prasad, *Chem. Eur. J.* **2008**, *14*, 5812–5819; g) O. Buyukcakir, O. A. Bozdemir, S. Kolemen, S. Erbas, E. U. Akkaya, *Org. Lett.* **2009**, *11*, 4644–4647; h) S. Atilgan, Z. Ekmekci, A. L. Dogan, D. Guc, E. U. Akkaya, *Chem. Commun.* **2006**, 4398–4400; i) T. Rohand, W. Qin, N. Boens, W. Dehaen, *Eur. J. Org. Chem.* **2006**, 4658–4663; j) O. A. Bozdemir, O. Buyukcakir, E. U. Akkaya, *Chem. Eur. J.* **2009**, *15*, 3830–3838; k) T. Rousseau, A. Cravino, T. Bura, G. Ulrich, R. Ziessel, J. Roncali, *Chem. Commun.* **2009**, 1673–1675; l) T. Rousseau, A. Cravino, T. Bura, G. Ulrich, R. Ziessel, J. Roncali, *J. Mater. Chem.* **2009**, *19*, 2298–2300; m) J. Y. Liu, E. A. Ermilov, B. Roder, *Chem. Commun.* **2009**, 1517–1519; n) S. L. Niu, G. Ulrich, R. Ziessel, A. Kiss, P. Y. Renard, A. Romieu, *Org. Lett.* **2009**, *11*, 2049–2052; o) Q. W. Wen, M. Baruah, M. Sliwa, M. van der Auweraer, W. M. de Borggraeve, D. Beljonne, B. van Averbeke, N. Boens, *J. Phys. Chem. A* **2008**, *112*, 6104–6114; p) S. Diring, F. Puntoriero, F. Nastasi, S. Campagna, R. Ziessel, *J. Am. Chem. Soc.* **2009**, *131*, 6108–6109; q) D. Kumaresan, R. P. Thummel, T. Bura, G. Ulrich, R. Ziessel, *Chem. Eur. J.* **2009**, *15*, 6335–6339.

[8] a) A. B. Descalzo, H. J. Xu, Z. L. Xue, K. Hoffmann, Z. Shen, M. G. Weller, X. Z. You, K. Rurack, *Org. Lett.* **2008**, *10*, 1581–1584; b) K. Umezawa, Y. Nakamura, H. Makino, D. Citterio, K. Suzuki, *J. Am. Chem. Soc.* **2008**, *130*, 1550–1551; c) Z. Shen, H. Röhr, K. Rurack, H. Uno, M. Spieles, B. Schulz, G. Reck, N. Ono, *Chem. Eur. J.* **2004**, *10*, 4853–4871; d) M. Wada, S. Ito, H. Uno, T. Murashima, N. Ono, T. Urano, Y. Urano, *Tetrahedron Lett.* **2001**, *42*, 6711–6713.

[9] a) Y. Zhou, Y. Xiao, S. Chi, X. Qian, *Org. Lett.* **2008**, *10*, 633–636; b) J. Feng, B. Liang, D. Wang, L. Xue, X. Li, *Org. Lett.* **2008**, *10*, 4437–4440.

[10] a) A. Coskun, M. D. Yilmaz, E. U. Akkaya, *Org. Lett.* **2007**, *9*, 607–610; b) A. Loudet, R. Bandichhor, L. X. Wu, K. Burgess, *Tetrahedron* **2008**, *64*, 3642–3654; c) W. Zhao, E. M. Carreira, *Chem. Eur. J.* **2006**, *12*, 7254–7263.

[11] a) A. Gorman, J. Killoran, C. O'Shea, T. Kenna, W. M. Gallagher, D. F. O'Shea, *J. Am. Chem. Soc.* **2004**, *126*, 10619–10631; b) S. O. McDonnell, D. F. O'Shea, *Org. Lett.* **2006**, *8*, 3493–3496; c) W. M. Gallagher, L. T. Allen, C. O'Shea, T. Kenna, M. Hall, A. Gorman, J. Killoran, D. F. O'Shea, *Br. J. Cancer* **2005**, *92*, 1702–1710; d) S. O. McDonnell, M. J. Hall, L. T. Allen, A. Byrne, W. M. Gallagher, D. F. O'Shea, *J. Am. Chem. Soc.* **2005**, *127*, 16360–16361; e) M. J. Hall,

L. T. Allen, D. F. O'Shea, *Org. Biomol. Chem.* **2006**, *4*, 776–780; f) J. Killoran, D. F. O'Shea, *Chem. Commun.* **2006**, 1503–1505; g) J. Murtagh, D. O. Frimannsson, D. F. O'Shea, *Org. Lett.* **2009**, *11*, 5386–5389; h) A. Palma, M. Tasior, D. O. Frimannsson, T. Truc Vu, R. Méallet-Renault, D. F. O'Shea, *Org. Lett.* **2009**, *11*, 3638–3641; i) M. Tasior, J. Murtagh, D. O. Frimannsson, S. O. McDonnell, D. F. O'Shea, *Org. Biomol. Chem.* **2010**, *8*, 522–525.

[12] a) W. Zhao, E. M. Carreira, *Angew. Chem.* **2005**, *117*, 1705–1707; *Angew. Chem. Int. Ed.* **2005**, *44*, 1677–1679; b) G. Sathyamoorthi, M. Soong, T. W. Ross, J. H. Boyer, *Heteroat. Chem.* **1993**, *4*, 603–608.

[13] V. F. Donyagina, S. Shimizu, N. Kobayashi, E. A. Lukyanets, *Tetrahedron Lett.* **2008**, *49*, 6152–6154.

[14] J. Killoran, L. Allen, J. Gallagher, W. Gallagher, D. F. O'Shea, *Chem. Commun.* **2002**, 1862–1863.

[15] W. M. Sharman, J. E. Van Lier in *The Porphyrin Handbook*, *Vol. 15* (Eds.: K. M. Kadish, K. M. Smith, R. Guilard), Academic Press, San Diego, **2003**, pp. 1–60.

[16] a) N. Kobayashi, J. Mack, K. Ishii, M. J. Stillman, *Inorg. Chem.* **2002**, *41*, 5350–5363; b) N. Kobayashi in *The Porphyrin Handbook*, *Vol. 15* (Eds.: K. M. Kadish, K. M. Smith, R. Guilard), Academic Press, San Diego, **2003**, pp. 161–262; c) T. Nonomura, N. Kobayashi, T. Tomura, *J. Porphyrins Phthalocyanines* **2000**, *4*, 538–543.

[17] a) R. Weiss, G. Schelsinger, *Monatsh. Chem.* **1927**, *48*, 451–457; b) H. Bredereck, H. W. Vollmann, *Chem. Ber.* **1972**, *105*, 2271–2283.

[18] A. Loudet, R. Bandichhor, K. Burgess, A. Palma, S. O. McDonnell, M. J. Hall, D. F. O'Shea, *Org. Lett.* **2008**, *10*, 4771–4775.

[19] A. Bondi, *J. Phys. Chem.* **1964**, *68*, 441–451.

[20] Ground-state dipole moments were calculated to be 0.0087 D for **2**, 2.5 D for **3** and 0.85 D for **5**.

[21] K. Umezawa, A. Matsui, Y. Nakamura, D. Citterio, K. Suzuki, *Chem. Eur. J.* **2009**, *15*, 1096–1106.

[22] a) Y. W. Wang, M. X. Yu, Y. H. Yu, Z. P. Bai, Z. Shen, F. Y. Li, X. Z. You, *Tetrahedron Lett.* **2009**, *50*, 6169–6172; b) S. Atilgan, T. Ozdemir, E. U. Akkaya, *Org. Lett.* **2008**, *10*, 4065–4067; c) S. Ozlem, E. U. Akkaya, *J. Am. Chem. Soc.* **2009**, *131*, 48–49.

[23] a) M. A. Robb, F. Bernardi, M. Olivucci, *Pure Appl. Chem.* **1995**, *67*, 783–789; b) M. Z. Zgierski, T. Fujiwara, E. C. Lim, *Chem. Phys. Lett.* **2008**, *463*, 289–299.

[24] M. Gouterman in *The Porphyrins*, *Vol. 3* (Ed.: D. Dolphin), Academic Press, New York, **1978**, pp. 1–156.

[25] *The Porphyrin Handbook*, Vol. 16 (Eds.: K. M. Kadish, K. M. Smith, R. Guilard), Academic Press, San Diego, **2003**.

[26] H. Stiel, K. Teuchner, A. Paul, W. Freyer, D. Leupold, *J. Photochem. Photobiol. A* **1994**, *80*, 289–298.

[27] G. M. Sheldrick, SHELXS-97 and SHELXL-97, Program for the Solution and Refinement of Crystal Structures, University of Göttingen, Göttingen, Germany, **1997**.

[28] X. G. Yadokari, Software for Crystal Structure Analyses, K. Wakita, (2001); Release of Software (Yadokari-XG 2009) for Crystal Structure Analyses, C. Kabuto, S. Akine, T Nemoto, E. Kwon, *J. Cryst. Soc. Jpn.* **2009**, *51*, 218–224.

[29] Gaussian 03, M. J. Frisch, G. W. Trucks, H. B. Schlegel, G. E. Scuseria, M. A. Robb, J. R. Cheeseman, J. A. Montgomery, J. T. Vreven, K. N. Kudin, J. C. Burant, J. M. Millam, S. S. Iyengar, J. Tomasi, V. Barone, B. Mennucci, M. Cossi, G. Scalmani, N. Rega, G. A. Petersson, H. Nakatsuji, M. Hada, M. Ehara, K. Toyota, R. Fukuda, J. Hasegawa, M. Ishida, T. Nakajima, Y. Honda, O. Kitao, H. Nakai, M. Klene, X. Li, J. E. Knox, H. P. Hratchian, J. B. Cross, C. Adamo, J. Jaramillo, R. Gomperts, R. E. Stratmann, O. Yazyev, A. J. Austin, R. Cammi, C. Pomelli, J. W. Ochterski, P. Y. Ayala, K. Morokuma, G. A. Voth, P. Salvador, J. J. Dannenberg, V. G. Zakrzewski, S. Dapprich, A. D. Daniels, M. C. Strain, O. Farkas, D. K. Malick, A. D. Rabuck, K. Raghavachari, J. B. Foresman, J. V. Ortiz, Q. Cui, A. G. Baboul, S. Clifford, J. Cioslowski, B. B. Stefanov, G. Liu, A. Liashenko, P. Piskorz, I. Komaromi, R. L. Martin, D. J. Fox, T. Keith, M. A. Al-Laham, C. Y. Peng, A. Nanayakkara, M. Challacombe, P. M. W. Gill, B. Johnson, W. Chen, M. W. Wong, C. Gonzalez, J. A. Pople, Gaussian, Inc., Wallingford CT, **2004**.

Received: September 4, 2010
Published online: March 4, 2011

